OUKA
The University of Osaka
Institutional Knowledge Archive

Title	Optical Interaction between Laser Beam and Induced Plume in the Ultra-High Power Density Fiber Laser Welding of Stainless Stee
Author(s)	Kawahito, Yousuke; Mizutani, Masami; Katayama, Seiji
Citation	Transactions of JWRI. 2008, 37(2), p. 19-25
Version Type	VoR
URL	https://doi.org/10.18910/5073
rights	
Note	

The University of Osaka Institutional Knowledge Archive : OUKA

https://ir.library.osaka-u.ac.jp/

The University of Osaka

Optical Interaction between Laser Beam and Induced Plume in the Ultra-High Power Density Fiber Laser Welding of Stainless Steel †

KAWAHITO Yousuke*, MIZUTANI Masami and KATAYAMA Seiji*****

Abstract

The objective of this research is to obtain a fundamental knowledge of the optical interactions in a 10-kW fiber laser beam of 0.9-MW/mm^2 power density and the plume or plasma induced during bead-on-plate welding of 20-mm-thick Type 304 stainless steel plate, on the basis of high-speed video observations, spectroscopic analysis and laser probe measurements. According to the high-speed observation results, the laser-induced plume was repeatedly generated from a keyhole at intervals of about 0.5-ms. The spectroscopy indicated that a bright plume emitted the line spectra of neutral atoms of alloying elements in Type 304 such as iron (Fe), chromium (Cr) and manganese (Mn). The temperature and the ionization degree of the laser-induced plume were calculated to be approximately 6,000 K and 0.02, respectively, by the Bolzman plots and via Saha's equation. Furthermore, the probe laser passed horizontally through the plume was refracted at 0.6-mrad angle on average, which was much lower than the 90-mrad divergence of the focused fiber laser beam. The attenuation of the probe laser was measured to be about 4 %, which was not mainly caused by Inverse Bremsstrahlung but by Rayleigh scattering. Subsequently, a stable laser welding process could be established at such an ultra-high power density that 11.5-mm-deep penetration was obtained even if the laser peak power was modulated 1-ms-periodically from 10 kW to 8.5 kW. It was consequently considered that the optical interaction between the 10-kW fiber laser beam and the weakly-ionized plume was too small to exert a reduction in weld penetration.

KEY WORDS: (High-power fiber laser), (Laser-induced plume), (Stainless steel), (high-speed observation), (Spectroscopic analysis), (Laser probe measurements)

1. Introduction

Recently, high-power fiber lasers and disk lasers have been receiving attention owing to their advantages such as beam quality superior to yttrium aluminum garnet (YAG) laser and carbon dioxide (CO_2) laser, as well as flexible fiber delivery due to their wavelengths of about 1 μm[1~3]. A 10-kW fiber laser beam is easily focused into about 100 μm in spot diameter, which can produce an ultra-high power density of about 1 MW/mm^2 class corresponding to a focused electron beam. Therefore, these high-brightness lasers have been regarded as new desirable heat sources for laser welding. However, only a few attempts have been made so far to clarify fundamental features of the optical interaction between the ultra-high power density fiber laser and the laser-induced plume.

It is well known that a deep weld penetration can be drastically reduced by the attenuation of an incident laser beam due to Inverse Bremsstrahlung of a plasma induced during welding with a high-power CO_2 laser beam in argon (Ar) shielding gas[4~12]. Moreover, the differential interferometry of the plasma indicated that the defocusing and deflecting effect derived from refraction of the plasma would strongly influence the stability of welding process due to a temporal as well as a spatial variation of laser power density on the sample surface[13]. On the other hand, the authors revealed that optical interaction of a plume induced by a 3-kW YAG laser beam with power density of 20 kW/mm^2 was too small to reduce weld penetration[14]. Such difference between two lasers is attributed to the ionized levels of the laser-induced plume and their wavelength.

In this research, a continuous wave (CW) fiber laser was utilized for bead-on-plate welding of a 20-mm-thick Type 304 stainless steel plate in Ar shielding gas. The maximum laser power and power density were 10 kW and 0.9 MW/mm^2, respectively. The generation behavior of the laser-induced plume was observed with a high-speed video camera of 40,000 frames/s. According to spectroscopic analysis of the

† Received on December 26, 2008
* Assistant Professor
** Technical Official
*** Professor

Transactions of JWRI is published by Joining and Welding Research Institute, Osaka University, Ibaraki, Osaka 567-0047, Japan

laser-induced plume, the temperature and the ionization degree were calculated on the basis of emission spectra, except self-absorption lines, by the Bolzman plots and via Saha's equation. Moreover, the refraction of the probe laser beam by the plume was measured on the basis of 10,000-frames/s-high-speed observation images of the probe laser spot behavior during welding. The attenuation was calculated by the decrease in the probe laser power during welding, and its dominant factor was determined by measuring the attenuation levels of other probe lasers with different wavelengths. Subsequently, the penetration depths were assessed by increasing the fiber laser power from 2 kW to 10 kW. The effect of the periodical generation of the laser-induced plume on the weld penetration was evaluated by comparing the weld penetrations produced by several kinds of power modulations of the 10-kW fiber laser.

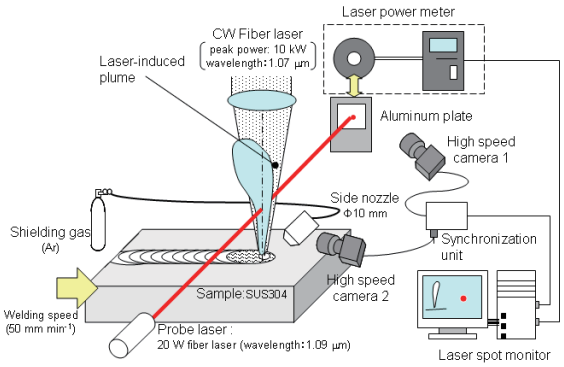

Fig. 1 Schematic experimental set-up of high-speed video observation and power measurement system for understanding the interaction between probe laser beam and plume during welding with 10-kW fiber laser.

2. Experimental set-up and materials used

The material used in this study is SUS 304 (Japanese Industrial Standard (JIS) corresponding to Type 304 or AISI 304) austenitic stainless steel of 20 mm in plate thickness. The laser apparatus used is (IPG) fiber laser machine of 1,070-nm wavelength and 10-kW-maximum power to confirm the formation of a weakly-ionized plume. A 10-kW fiber laser beam was delivered through the optical fiber and was focused into a spot of 130 μm diameter by a lens of 150-mm-focal distance, which produced the ultra-high power density of 0.9 MW/mm^2. A Type 304 plate was welded at the focal position in Ar shielding gas of 30 L/min flow rate as illustrated in **Fig. 1**. The welding speed was 50 mm/s and the shielding gas nozzle position was 10 mm above the sample surface.

The ionization level of the laser-induced plume was investigated by spectroscopic measurement using the diffraction gratings of 150 and 1200 gr/mm for broad and narrow spectrum bands, respectively. The spectroscope had the measurement area of 500 μm in spot diameter at 2-mm height above the sample plate surface, and a long wave pass filter of less than 750 nm was utilized to cut off the high-order diffracted light in the spectroscopic measurement of 800 nm to 850 nm in wavelength. All the measured wavelengths were calibrated from the references of both a mercury lamp and a spectral irradiance standard lamp. The integration time for the spectroscopic measurements was 50 ms. As for laser probe measurements, the observation spot was located at 2 m away from the focused laser beam in order to attenuations of the probe laser were measured at several probe positions with a commercially available power meter. The probe lasers used were fiber, diode and Helium-Neon (He-Ne) lasers of 1,090 nm 830 nm and 633 nm in wavelength, respectively. Moreover, the effect of a weakly-ionized plume on weld penetration was investigated under the laser power conditions of 2 kW to 10 kW and several laser power modulations at 500-Hz cycles.

3. Experimental results and discussion

3.1 Features of the plume induced with a 10 kW fiber laser beam

Bead-on-plate welding was performed on the stainless steel plate of 20 mm in thickness with a 10-kW fiber laser beam of 0.9-MW/mm^2 power density under Ar shielding gas. The penetration was approximately 12 mm and stable in the welding direction. Then the laser-induced plume was observed by a high-speed video camera at the framing rate of 40,000 frames/s. The typical picture obtained is shown in **Fig. 2**. A blue emitted plume was generated after 0.5 s from the laser irradiation. It grew up to about 2 mm in height above the plate surface after 125 μs, where the emission was the brightest. Thereafter the blue emitted plume changed to

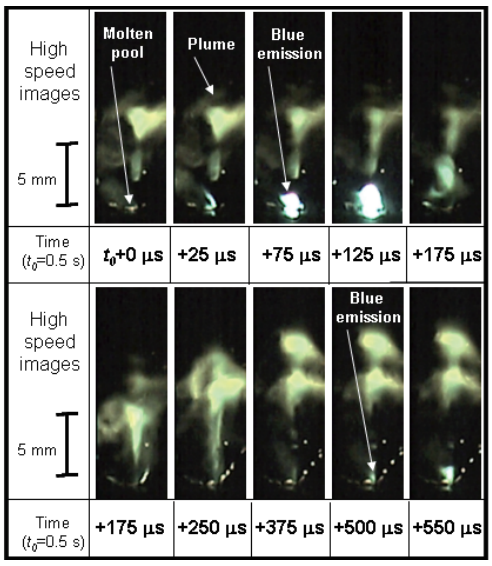

Fig. 2 Series of 40,000-frames/s-high speed video images of plume growth generated by 0.9-MW/mm^2-focused 10 kW fiber laser beam in Ar shielding gas.

a reddish one, whose top reached 12 mm after 375 μs. After 500 μs, the blue emitted plume was observed again as well as before 500 μs. The plume was generated periodically at about 500-μs cycles.

The ionization degree of the laser-induced plume with blue emission was analyzed by spectroscopy. Then spectroscopic analysis was exploited in broad spectrum bands of 300 nm to 800 nm in wavelength. The result obtained at the laser powers of 10 kW is shown in **Fig. 3**. According to the spectroscopic measurement results the intensity of the neutral line spectra of Fe, Cr and Mn peaked between 358 nm and 495 nm. Therefore, the blue emitted plume observed at 10 kW was attributed to their line spectra. The detailed results of spectroscopic analyses of plume induced at 10 kW at 430 nm to 470 nm in wavelength and 800 nm to 850 nm are represented in **Fig. 4** (a) and (b), respectively. All the measured line spectra were identified from the tables of spectrum lines[15]. Fig. 4 (a) shows that all the emission of the laser-induced plume are derived from line spectra of neutral atoms such as Fe, Cr and Mn which are alloying elements of SUS 304. However, although the region of the spectroscopic measurement included the high intensity of Fe ion spectrum of 458.384 nm in wavelength, ion spectra of alloying elements and line spectra of an argon neutral atom were not detected. The results were similar to those in other wavelength regions which included some strong line spectra of Ar neutral atom such as 811.531 nm or 840.821 nm as shown in Fig. 4 (b).

3.2 Measurements of temperature and ionization degree of 10 kW fiber laser induced plume

The temperature and the ionization degree of the laser-induced plume at 10-kW laser power were calculated on the basis of the relative intensity of the line spectra obtained from the above-mentioned spectroscopic measurement results. Here, the temperature and the ionization degree were average values among five spectroscopic measurements with the exposure time of 50 ms and the measurement area of 500 μm in spot diameter at 2-mm height above the laser-irradiated plate surface. The plume temperature was determined by the following equation on the assumption that the plume was in local thermal equilibrium.

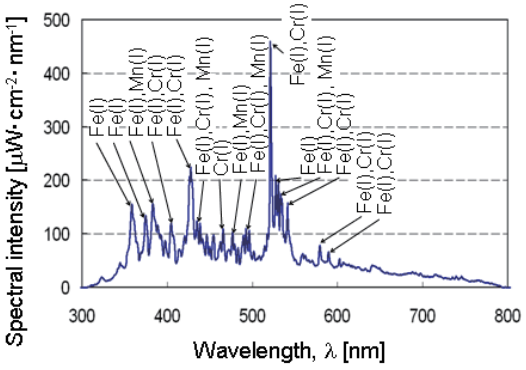

Fig. 3 Spectroscopy of plume induced during welding with 10 kW fiber laser in Ar shielding gas.

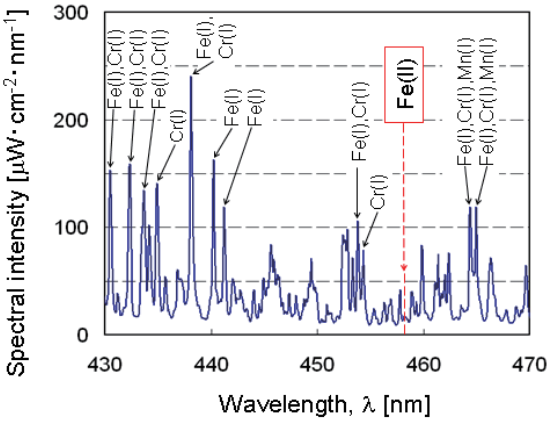

(a) Spectroscopy between 430 nm and 460 nm wavelengths

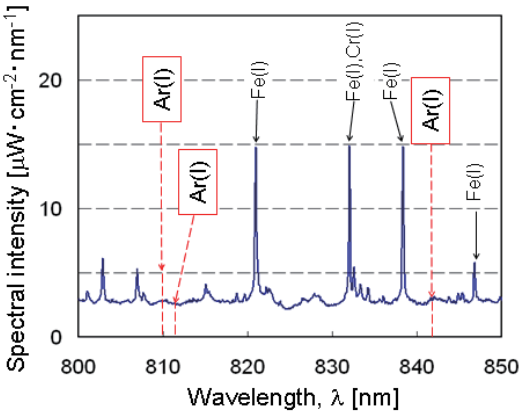

(b) Spectroscopy between 800 nm and 850 nm wavelengths

Fig. 4 Spectroscopy of 10-kW fiber laser induced plume in narrow wavelength bands.

$$In\left(\frac{I_{nm}\lambda_{nm}}{g_n A_{nm}}\right) = -\frac{E_n}{kT} + In\left(\frac{N_0 hc}{Z(T)}\right) \qquad (1)$$

where, N_0: atomic number density
E_n: excited energy at n-th level
λ_{nm}: wavelength emitted by n-m transition
$I_n m$: spectral line intensity of n-m transition
A_{nm}: transition probability from n-th to m-th level
g_n: statistical weight at n-th level
$Z(T)$: partition function of atom at temperature T
k: Boltzmann constant
h: Planck constant
c: velocity of light

Figure 5 shows the Boltzmann plots of measured intensities of spectral lines in different wavelengths, except the self-absorption lines. Here, the values of statistical weight and transition probability are quoted

form the handbook[16]. The temperature was determined to be about 6,000 K from the gradient of Boltzmann plots by the method of least squares. 6,000 K was lower than the temperatures of 8,000 K to 9,200 K reported concerning plasma in high-power CO_2 laser welding of stainless steels[17].

Subsequently, the ionization degrees of Fe and Ar were calculated by Saha's equation under the gas pressure of 760 Torr as shown in the following.

$$\frac{\alpha^2}{1-\alpha^2} = \left(\frac{2\pi m}{h^2}\right)^{\frac{3}{2}} \frac{(kT)^{\frac{5}{2}}}{p} \exp\left(-\frac{eV_i}{kT}\right) \qquad (2)$$

where, α: ionization degree
m: mass of electron
V_i: ionized voltage of gas
e: electronic charge
p: gas pressure

Figure 6 shows the calculated ionization degree of Fe and Ar as a function of temperature. Here, ionized voltages of Fe and Ar are 7.78 V and 15.76 V [18, 19], respectively. The ionization degree of the plume at 6,000 K was 0.02, as indicated in Fig. 6. Therefore, it was concluded that the laser-induced plume was heated to such a high temperature as to be a weakly-ionized plume.

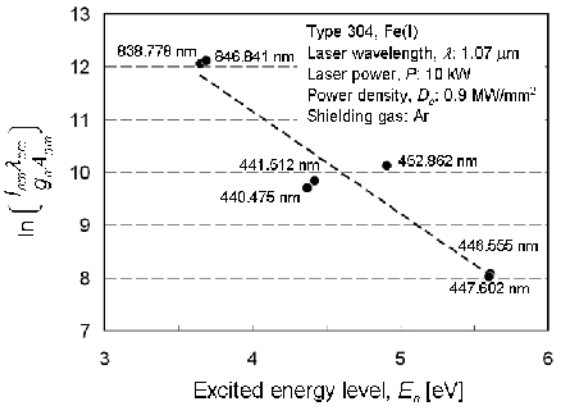

Fig. 5 Boltzmann plots of seven Fe (I) spectral lines of 10 kW fiber laser-induced plume from Type 304.

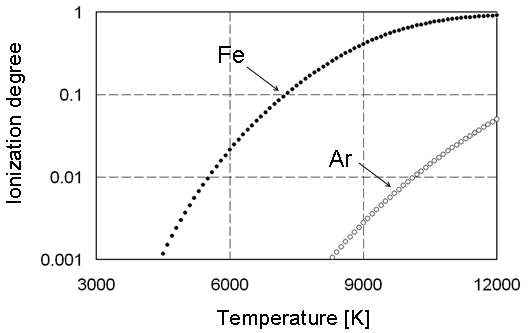

Fig. 6 Temperature dependence of ionization degree of Fe and Ar.

3.3 Refraction of fiber probe laser passing through weakly-ionized plume

In order to understand the refraction of a laser beam passing through the weakly-ionized plume, the spot behavior of the probe fiber laser beam passing horizontally through the high-power density fiber-laser-induced plume was observed with a 10,000-frames/s-high-speed video camera. The beam diameter and height of the probe laser were 0.8 mm and 3 mm above the sample surface, respectively. Simultaneous observation images of plume and probe laser spot behavior are shown in **Fig. 7**. 0 s is the start time of 10-kW fiber laser irradiation. The plume grew up to the height of 15 mm and showed various shapes. Correspondingly, the probe laser spot changed its size, shape, brightness and position. It was clearly confirmed that the probe fiber laser beam was refracted and attenuated by the laser-induced plume. However, it was difficult to identify a clear correlation between the plume and the probe laser spot from the 10,000-frames/s-high-speed video images.

Subsequently, the spot movement of the probe laser was investigated in detail. Considering that the spot shape was almost circular during welding, the spot position was represented by the weighted center of brightness in the probe laser spot. The spot movement represents the refraction angle which is defined by the arctangent of travel distance of the probe laser spot divided by 2-m distance between the laser irradiation point and the observation position. **Figure 8** demonstrates the refraction angles obtained during the laser irradiation of 0.9 s to 1.3 s when the plume was periodically generated and a smaller amount of spatter occurred. The weld of 20 mm in length was produced at the welding speed during 0.4-s period. Original central point stands for the spot position before the 10-kW fiber laser irradiation. The probe laser beam was refracted in

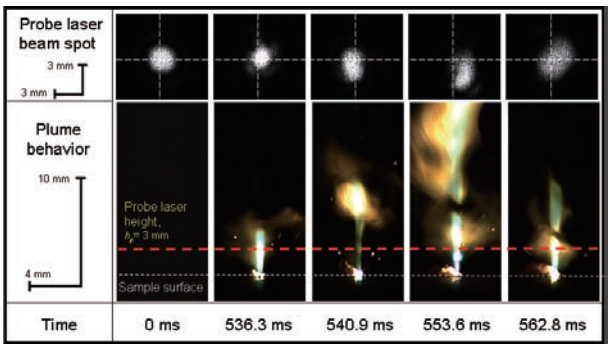

Fig. 7 10,000-frames/s-high-speed video pictures during high power fiber laser welding, showing rapid behavior of laser-induced plumes and corresponding shifts in probe fiber laser beam spots.

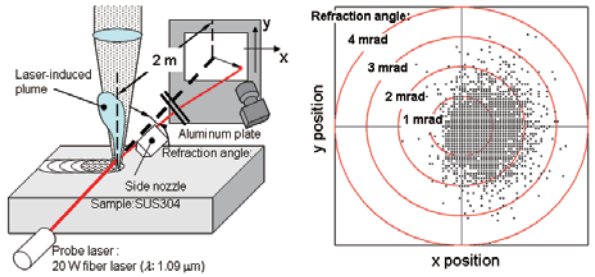

Fig. 8 Schematic of experimental set-up and shifted spot location and distribution of probe fiber laser beam passing through the plume at 3-mm height at 30-L/min flow of Ar shielding gas from side nozzle.

various directions by the plume, and the refraction angles had a wide distribution due to several directions of the spot shifts. The average refraction angle is 0.4 mrad. The refraction of the probe laser inclined on the whole to a shielding gas nozzle.

Moreover, the average refraction angles at the probe laser height of 3 mm, 10 mm and 15 mm are summarized in **Table 1**. The maximum angle is 0.6 mrad at 10 mm, which is much lower than about 90-mrad beam divergence of the 10-kW fiber laser used. When an incident beam of fiber laser was bent at 0.6 mrad angle at 10 mm height above sample surface, the laser spot diameter could expand about 6 μm wider, which was negligible in comparison with 130 μm in laser spot diameter. It was revealed that the refraction angle increased with the decrease in the molecular weight of the shielding gas in the case of a 3-kW-YAG-laser-induced plume (negligibly or non-ionized plasma)[14]. Taking into account that the probe laser height of 10 mm is the same position as the shielding gas nozzle, it is considered that the probe laser is refracted at the boundary between high temperature of the weakly-ionized plume and room temperature of the shielding gas.

3.4 Attenuation of probe fiber laser power passing through weakly-ionized plume

Attenuation is defined as the ratio of the decrease in probe fiber laser power during the welding to the initial power. The measurement powers at the probe laser height of 3 mm are shown in comparison with the longitudinal cross section of the weld bead in **Fig. 9**. It shows that the laser power was 1.03 W before laser irradiation and dropped down to 0.96 W at the minimum. The probe power was raised again to 0.99 W during the laser irradiation of 0.9 s to 1.3 s when a smaller amount of spatter occurred, the decreased probe laser power was stably constant, and the minimum penetration depth of 11.7 mm was the same. Therefore, the attenuation values during the laser irradiation period of 0.9 s to 1.3 s were selected and compared. The attenuation was calculated to be 4 %. Moreover, the attenuations of 3 mm, 10 mm and 15 mm in the probe laser height are summarized in **Table 2**. The attenuation decreased as the probe laser height approached the top position of the plume. At 15 mm the attenuation was negligible. It was found that the maximum attenuation was 4 % at 3-mm probe laser height, which was as low as 2 % power variation for the incident 10-kW fiber laser.

There are some kinds of attenuation factors such as Rayleigh scattering and Inverse Bremsstrahlung which are proportional to the wavelength to the power of minus four and plus two, respectively. Therefore, the attenuation factor was identified by additionally using He-Ne and a diode laser as a probe laser beam. **Figure 10** shows relative attenuation per unit area of probe laser beams. The attenuation is defined as a value divided by the respective diameter of the probe laser. Each probe

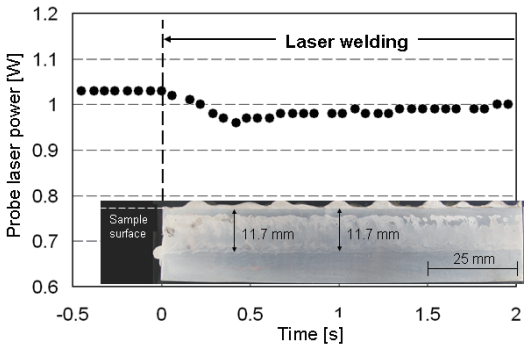

Fig. 9 Attenuation measurement of probe laser at 3-mm height shown as function of longitudinal cross section of weld bead.

Table 1 Average refraction angle of probe laser beam as function of measurement height during welding with 10-kW fiber laser.

Height of probe laser	Average refraction angle
3 mm	0.4 mrad
10 mm	0.6 mrad
15 mm	0.1 mrad

*probe beam diameter: 0.8 mm

Table 2 Attenuation of probe laser power as function of measurement height during welding with 10-kW fiber laser.

Height of probe laser	Attenuation of probe laser power
3 mm	4 %
10 mm	1.9 %
15 mm	0 %

*probe beam diameter: 0.8 mm

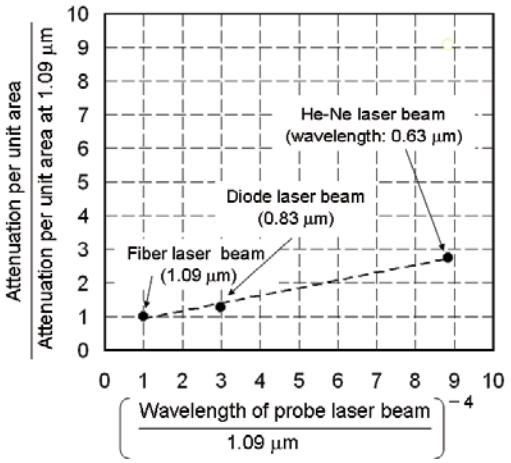

Fig. 10 Correlation of laser-induced plume or plasma at focal position to relative attenuation in probe laser beams of different-wavelengths.

laser wavelength is also divided by 1,090-nm wavelength, and then the ratio raised to minus fourth power is selected as the horizontal axis. The vertical axis is the ratio of the attenuation per unit area of each probe laser to the 1,090-nm-wavelength probe fiber laser. The graph indicates that the attenuation is in proportion to the wavelength to the minus fourth power. The main attenuation factor is therefore attributed not to Inverse Bremsstrahlung but Rayleigh scattering. However, the attenuation appears to be caused partly by absorption and reflection due to spatter, judging from the result that the greater power attenuation occurred during severe spattering in the initial stage of welding.

3.4 Effect of a weakly-ionized plume on weld penetration

It was confirmed in the above experiment that the weakly-ionized plume exerted a smaller effect on refraction or attenuation of the probe fiber laser passing horizontally above the sample surface. Subsequently, the effect of weakly-ionized plume on weld penetration was investigated at several constant and modulated laser powers. The bead-on-plate welding of 20-mm-thick stainless steel plates was exploited with laser power of 2 kW to 10 kW. The relationship between laser power and penetration depth is shown in **Fig. 11**. The penetration became deeper from 4 mm to 11.5 mm as the laser power increased, which indicates that the penetration is almost proportional to the laser peak power. In high-power CO_2 laser welding in Ar shielding gas, it was reported that a deep weld penetration could be drastically reduced by attenuation of an incident laser beam due to Inverse Bremsstrahlung of a laser-induced plasma with more than 0.65 in ionization degree[7]. Therefore, the weakly-ionized plume with about 0.02 ionization degree does not seem to greatly exert the reduction in weld penetration.

Figure 12 demonstrates the longitudinal cross sections produced with or without the laser power modulations under the consideration of the fact that the laser-induced plume or plasma is generated at the cycle of 500 ms to 2 ms. The peak power is modulated from 10 kW to laser base power P_{base} of 5 kW to 9.5 kW at an interval of 1 ms. The horizontal axis is laser base power P_{base}. The vertical axis is the ratio R_c of the average penetration with the laser power modulation under the conventional welding conditions. Here the average penetration depth is defined by the 5-mm longitudinal cross section area of the weld metal (except humping parts) divided by 5 mm. The average penetration depths maintained the conventional ones at more than 8.5 kW in P_{base}. But at P_{base} of 5.5 kW, the value of R_c was below 90 % and the unstable penetrations with spiking were formed. The spiking seems to derive from the unstable keyhole behavior.

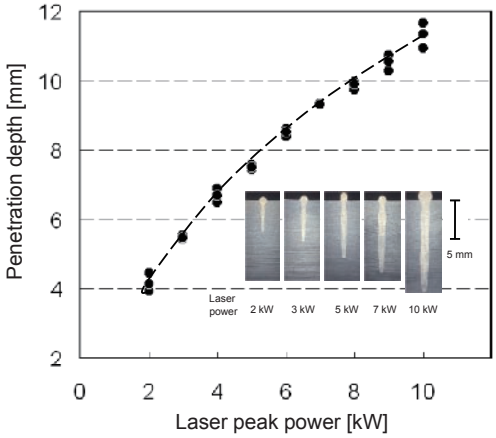

Fig. 11 Penetration depth of Type 304 weld bead as function of fiber laser peak power.

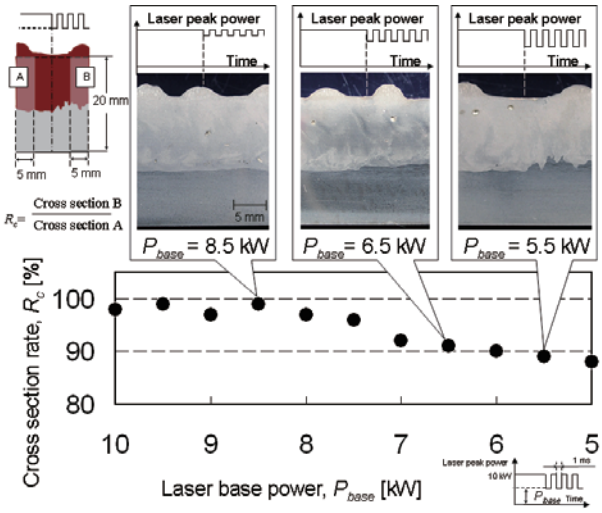

Fig. 12 Longitudinal cross sections of weld beads, and decrease in penetration at modulated laser peak power.

It was consequently considered that the optical interaction between the 10-kW fiber laser beam and the weakly-ionized plume was too small to exert the reduction in weld penetration.

5. Conclusions

A fundamental knowledge was obtained from the optical interaction of a fiber laser beam through a weakly-ionized plume induced during bead-on-plate welding of 20-mm-thick Type 304 plates with a 10-kW laser beam and the ultra-high power density of 0.9 MW/mm^2. According to the high-speed observation pictures, the laser-induced plume was repeatedly generated from a keyhole at the interval of about 0.5-ms period. The spectroscopy indicated the line spectra of neutral atoms of alloying elements of Type 304 such as iron (Fe), chromium (Cr) and manganese (Mn). The temperature and the ionization degree of the laser-induced plume were calculated to be approximately 6,000 K and 0.02, respectively, by the Bolzman plots and via Saha's equation. Furthermore, The probe laser measurement results revealed that the average refraction and attenuation were less than 0.6 mrad and 4 %, which were lower than or almost the same levels as the laser beam parameters such as beam divergence and power variation of the incident 10-kW laser beam, respectively. The main attenuation factor was attributed not to Inverse Bremsstrahlung but Rayleigh scattering. Subsequently, a stable laser welding process could be produced at such ultra-high power density that 11.5-mm-deep penetration was obtained even if the laser peak power was modulated 1-ms-periodically from 10 kW to 8.5 kW. It was consequently considered that the optical interaction between the 10-kW fiber laser beam and the weakly-ionized plume was too small to exert a reduction in weld penetration.

Acknowledgements

This work was conducted as part of the project, "Development Base of Joining Technology for New Metallic Glasses and Inorganic Materials" (DBJT) cooperated by three Research Institutes such as Joining and Welding Research Institute (JWRI) of Osaka University, Institute for Material Research (IMR) of Tohoku University and Materials and Structures Laboratory (MSL) of Tokyo Institute of Technology. The authors would like to acknowledge Mr. Keisuke Kinoshita and Mr. Naoyuki Matsumoto, former graduate students of Mechanical Engineering Course of Osaka University, for their help in some experiments.

References

1) E. Beyer, B. Brenner, A. Klotzbach and S. Nowotny: Online Proc. the 4th International Congress on Laser Advanced Materials Processing, 2006, #06-1.
2) F. Vollertsen: Online Proc. the 4th International Congress on Laser Advanced Materials Processing, 2006, #06-188.
3) J. Weberpals, C. Deininger and F. Dausinger: Online Proc. the 4th International Congress on Laser Advanced Materials Processing, 2006, #06-2.
4) E. V. Locke, E. D. Hoag and R. A Hella: Quantum Electronics, IEEE Journal, 1972, 8, pp.132-135.
5) E. Beyer, K. Behler and G.. Herziger: SPIE, 1988, 1020, pp.84-95.
6) T. Ishide, S. Shono, T. Ohmae, H. Yoshida and A. Shinmi: LAMP '87, JLPS, Osaka, 1987, pp.187-191.
7) M. Ono, K. Nakada and S. Kosuge: Q. J. of JWS, 1992, 10, pp.239-245.
8) R. Fabbro: LAMP '92, JLPS, Nagaoka, 1992, pp.305-310.
9) I. Miyamoto and H. Maruo: LAMP '92, JLPS, Nagaoka, 1992, pp.311-322.
10) A. Poueyo, G. Deshors, R. Fabbro, A. M. de Frutos and J. M. Orza: LAMP '92, JLPS, Nagaoka, 1992, pp.323-328.
11) S. Tsukamoto: J. of JLPS, 2001, 8, pp.37-41.
12) N. Seto, S. Katayama and A. Matsunawa: J. Laser Applications, 2000, 12, pp.245-250.
13) H. Schittenhelm, J. Muller, P. Berger and H Hugel: Section E - ICALEO 1999, LIA, San Diego, 1999, pp.195-204.
14) Y. Kawahito, K. Kinoshita, S. Katayama, S Tsubota and T. Ishide: Journal of JLPS, 2006, 13, pp.41-47.
15) A. N. Zaidel', V. K. Prokof'ev and S. M. Raiskii: Tabeles of specrum lines, Pergamon, 1961, pp.295-373.
16) C. H. Corliss and W. R. Bozman: Experimental transition probabilities for spectral lines of seventy elements, NBS Monograph, 1962, 53, pp.95-108.
17) R. Miller and T. DebRoy: J. Applied Physics, 1990, 68, pp.2045-2050.
18) S. Teii: Plasma fundamental engineering, Uchida Rokakuho, 1997, pp.89-99.
19) National Astronomical Observatory: Chronological scientific tables, Maruzen, 1994, pp.542-543.